Journal of Physical Sciences, Vol. 23, 2018, 209-215
ISSN: 2350-0352 (print), www.vidyasagar.ac.in/publication/journal
Published on 24 December 2018

Magnetic and Structural Investigation of $Ni_{1-x}Zn_xFe_2O_4$ (x = 0, 0.6, 0.8, 1) Spinel Ferrite Synthesized by Sol-Gel Auto Combustion Method.

S. A. Tirpude[1], N.N. Sarkar[2], P. S. Sawadh[3] and K.G. Rewatkar[4]

[1,3]Department of Applied Physics, B.D College of Engineering, Sevagram
Wardha, (M. S) – 442102, India
[2,4] Department of Physics, Dr. Ambedkar College, Deekshabhoomi
Nagpur (M. S.)- 440010, India
E-mail: sarkariresearch@gmail.com

Received 16 June 2018; accepted 1 December 2018

ABSTRACT

Ferrite samples of $Ni_{1-x}Zn_xFe_2O_4$ (x = 0, 0.6, 0.8, 1) nanoparticles were synthesized by the sol-gel auto-combustion technique. The goal of this research module is to evaluate the structural and magnetic properties of Ni^{2+} and Zn^{2+}doped ferrite. X-ray diffraction (XRD) and vibrating sample magnetometer (VSM) analysis were carried out in order to characterize the structural and magnetic properties of synthesizing nanoparticles. The XRD results confirmed the formation of a single phase of spinel ferrite particles for an entire series of the material. The particle size was found to be nanometer range around 20 - 30 nm. The lattice parameter also calculated using XRD interpretation and the cation distribution also discuss briefly in the present research module. It was found that with an increase in substitution contents of Zn^{2+} ions the magnetization goes on decreases this may be due to the occupation of Zn^{2+} cations at both the site of octahedral and tetrahedral which causes to vary the magnetic interaction.

Keywords: XRD, VSM, Magnetic, structural, Cation distribution

1. Introduction

Ferrites are a special class of magnetic material made of metal oxides and ferric oxides, which is in the form of their main compositions [11]. The magnetic, electrical and dielectric properties of ferrite have made more attractive in the recent field of science and technology because of these novel properties of ferrite [2]. It is applicable in magnetic switches, microwave devices, microelectronic devices, sensors, electromagnetic circuits, transformer core, antenna rods and in the field of biomedical [3]. These properties are strongly dependent on a method of synthesis, the composition of chemicals, grain size and surface morphology etc. [4] Ferrites is broadly divided into two categories 'soft-ferrite' and 'hard ferrite' depending on the magnetic properties it is different in many cases, such as structural, chemical composition, magnetic and electrical properties. The soft ferrite is the materials that are magnetized and easily demagnetize, whereas hard ferrites are those that are difficult to make magnetic and demagnetize [5]. In the present research module we are deal with spinel type soft ferrite with the chemical composition of $Ni_{1-x}Zn_xFe_2O_4$ (x = 0, 0.6, 0.8, 1)

2. Experimental

2.1. Materials

The raw materials used for sol-gel auto combustion synthesis of $Ni_{1-x}Zn_xFe_2O_4$ (x = 0, 0.6, 0.8, 1) nanoparticles were Nickel nitrate (Ni $(NO_3)_2.6H_2O$), Zinc nitrate (Zn $(NO_3)_2.6H_2O$), ferric nitrate (Fe $(NO_3)_3.9H_2O$), Urea (NH_2-CO-NH_2). All the reagents used for the synthesis of cobalt ferrite nanoparticles were analytical grade.

2.2. Synthesis

$Ni_{1-x}Zn_xFe_2O_4$ (x = 0, 0.6, 0.8, 1) nanoparticles were synthesized by sol-gel auto combustion method using urea as a fuel. The stoichiometric proportions of metal nitrates were taken into separate glass beakers. These were stirred for 30 minutes to dissolve completely into the double distilled water. After complete dissolution, they were mixed properly. Then the solution was regularly stirred using magnetic stirrer and heated at 70-80 ^oC for 4h on a hot plate. Slowly it converts into viscous gel, and then the gel was kept in a microwave oven for an instant fire at 600 watts for maximum 5 to 10 min. The dried gel started and finally, the powder was obtained. The as-prepared ferrite powder was ground for 4 hrs and annealed at 800 ^oC for 4 hrs in a muffle furnace.

2.3. Characterizations

In the present work, Nickel Zinc substituted spinel ferrite samples were synthesized by sol-gel auto combustion method and characterized by X-ray diffraction technique and Vibrating sample magnetometer. X-ray diffraction patterns of all the samples were recorded in the 2θ verses intensity count with a scanning rate of 1.98 degrees per minute using Cu-Kα radiation of 1.5406 Å wavelength. The effect of substitution of divalent Zinc into the Nickel substituted spinel ferrite on the structural and magnetic behavior etc. was studied using XRD machine and VSM machine.

3. Results and discussion

3.1. XRD (x-ray diffraction)

The x-ray diffraction pattern of the sintered Ni^{2+} - Zn^{2+}doped spinel ferrite nano particle as shown in figure 1, from the (h k l) planes (1 1 1), (2 2 0), (3 1 1), (4 0 0), (4 2 2), (5 1 1), (4 4 0) (6 2 2) and (5 3 3), we confirming the single-phase cubic spinel structure of prepared sample [6]. The lattice parameter and their respective crystalline size were mentioned in table 1. The average crystallite size was calculated using Scherer's formula [7]. We notice that the lattice parameter increase gradually with the substitution of Zn^{2+} ions, this may be due to the large ionic radius of Zn^{+2} (0.74 Å) as compare to Ni^{+2} (0.70Å). In Fig. 1, the shift of (3 1 1) plane with the increase of Zn^{2+}content to the smaller diffraction angles indicating that the sample with higher Zn^{2+}concentration has a larger lattice parameter [8]. This is attributed to the fact of different radius of $Zn^{2+}$and Ni^{2+} cations which means that the larger the ionic radii larger are the lattice parameter [9]. Particle size was observed to decrease with the increasing addition of Zn^{2+}ions. The cation distribution has been calculated manually by using X-ray diffraction data. We observed Fe^{3+} cations were occupied mostly in tetrahedral sites showing almost an inverse-spinel type structure. Zn^{+2} ions are known to occupy tetrahedral (A) sites, as well as Octahedral B site due to their strong preference for octahedral coordination the distribution of Zn^{2+}ions, is more at B site [10]. The distribution of catio is shown in table

1. These results are proved to be consistent with the results of magnetic measurements. The cation distribution in $Ni_{1-x}Zn_xFe_2O_4$ (x = 0, 0.6, 0.8, 1) can be deduced from the X-ray diffraction technique comparative intensity calculated by using the following formula expressed by Buerger [11]

$$I_{h\,k\,l} = |F|^2 P L_P \tag{1}$$

where F is known as structure factor, and multiplicity factor denoted by P, L_p consider as Lorenz-polarization factor which depends on Bragg's diffraction angle θ

$$L_P = \frac{1+Cos^2 2\theta}{Sin^2\theta \cos\theta} \tag{2}$$

The formulae for the multiplicity factor and Lorentz polarization factor are taken from the literature [1, 12]. The structure factor (F) for various elements (Fe, Ni, Zn and O) were obtained from the literature [1, 12].

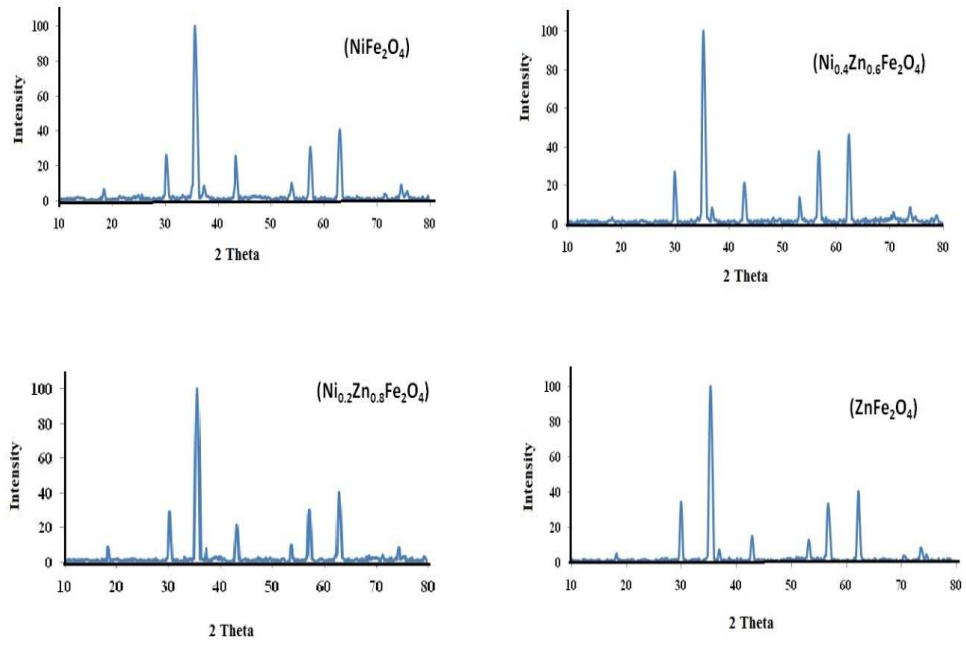

Figure 1: XRD pattern of $Ni_{1-x}Zn_xFe_2O_4$ (x = 0, 0.6, 0.8, 1)

Sr. No.	Sample	Crystalline size (nm)	Lattice parameter (Å)
1	$NiFe_2O_4$	33	8.4061
2	$Ni_{0.4}Zn_{0.6}Fe_2O_4$	30	8.3910
3	$Ni_{0.2}Zn_{0.8}Fe_2O_4$	28	8.3717
4	$ZnFe_2O_4$	26	8.3701

Table 1: XRD data

3.2. VSM (Vibrating Sample Magnetometer)

Fig. 2 shows the hysteresis loops of $Ni_{1-x}Zn_xFe_2O_4$ (x = 0, 0.6, 0.8, 1) ferrite nano-powders. The Saturation magnetization (Ms) and coercivity (Hc) of nano-powders as a function of Zn^{2+}substitution in Nickel ferrite are shown in Fig 2. Ms decreases gradually with the increase of Zn^{2+}substitution because Zn^{2+}has no magnetic moment [13]. Magnetic properties of ferrites are sensitively dependent on the structure, composition, defects, crystallite size, internal strain and cation distribution [14]. The magnetic moment of cubic spinel ferrite can be calculated by MB − MA, where MA and MB are the magnetizations of A and B-sites respectively, also the magnetic moment calculated using equation number 3 which is well agreement with each other and mention in table number 2.

$$\mu_{B=} \frac{Moleculer\ weight \times M_S}{5585} \quad (3)$$

The calculated magnetron number using XRD data is nearer to experimental data obtained from VSM which confirms the collinear magnetic structure in Zn^{2+}doped Ni spinel type ferrites [15]. Since the substituting Zn^{2+}ion occupied at A site and B site play an important role for the magnetization of material. The inherent magnetic moment of Fe^{3+} is $5\mu_B$, Ni^{2+} is 2 μ_B and for Zn^{2+} is 0 μ_B [16]. But when we pay attention to the cationic distribution, then we found that Ni^{2+} and Fe^{3+} ions both are distributed on tetrahedral and octahedral sites for the value of x = 0 [17] [18]. We also notice that the content of Ni^{2+} ions occupy less at A site and Fe^{3+} distributed in the ratio of 1:2 hence the Fe^{3+} is highest for the X = 0 value and lowest for x = 1 and hence the magnetization is large for nickel ferrite and vice versa for zinc ferrite is lowest [19] [20].

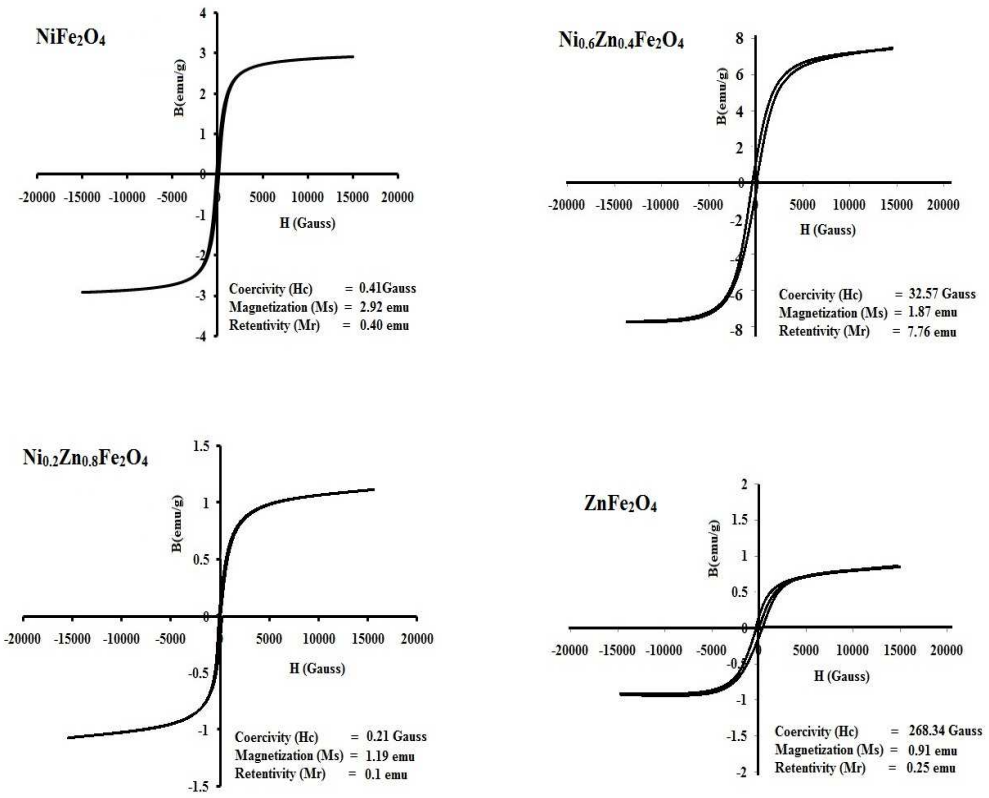

Figure 2: Magnetization behavior of $Ni_{1-x}Zn_xFe_2O_4$ (x = 0, 0.6, 0.8, 1)

Sr No.	$Ni_{1-x}Zn_xFe_2O_4$ composition (x)	Cation Distribution	Magnet-ization (emu)	Magne-tron number (μ_B)from XRD	Magne-tron number (μ_B) from VSM
1	0	$(Ni_{0.41}Fe_{0.95})$ $[Ni_{0.59}Fe_{1.05}]$	2.92	0.86	0.1225
2	0.6	$(Ni_{0.21}Zn_{0.06}Fe_{0.99})[Ni_{0.19}Zn_{0.54}Fe_{1.01}]$	1.87	0.06	0.0798
3	0.8	$(Ni_{0.11}Zn_{0.00}Fe_1)[Ni_{0.09}Zn_{0.80}Fe_1]$	1.19	0.04	0.0511
4	1	$(Zn_{0.01}Fe_{0.999})$ $[Zn_{0.99}Fe_{1.001}]$	0.91	0.01	0.0043

Table 2: Agreements of cationic distribution and magnetic moment

4. Conclusion

The magnetic material $Ni_{1-x}Zn_xFe_2O_4$ (x = 0, 0.6, 0.8, 1) has been successfully synthesized by sol-gel auto combustion method and characterized through XRD and VSM. With the help x- ray diffraction study we conclude that the prepared synthesized material is belong to space group Fd3m having single phase cubical structure. We may also conclude that the lattice parameter is directly proportional to ionic radii as we found in the present research module the lattice parameter increases with increasing ionic radii. The VSM study reveals B-H curve which is close resemble to super-paramagnetic in nature because the area of loop is very small but the coercivity (Hc) could not found to be zero since the material is not exactly super-paramagnetic in nature. The saturation magnetization is decreases with increasing Zn^{2+}concentration in the material, Nickel ferrite alone having highest magnetization and in addition to Zn^{2+}in Nickel ferrite the magnetization is fall down and finally the magnetization of Zn^{2+}ferrite alone is lowest. The value of magnetization and magnetron number calculated from VSM and XRD cation distribution is having good agreement with each other

Acknowledgement. The authors are thankful to the reviewers for their suggestions towards improvement of the paper.

REFERENCES

1. B.D.Cullity, Elements of X-Ray Diffraction. Addison-Wesley Publishing Company, 1 (1956) 333-340.
2. H.I.Gul, Electrical and magnetic characterization of nanocrystalline Ni–Zn ferrite synthesis by co-precipitation route, Journal of Magnetic Material, 320 (2008) 270–275.
3. V.G.Harris, Recent advances in processing and applications of microwave ferrites, Journal of Magnetic Material, 321 (2009) 2035–2047.
4. B.P.Jacob, Influence of preparation method on structural and magnetic properties of nickel ferrite nanoparticles, Bulletin. Material. Science, 34 (2011) 1345–1350.
5. H.Kavas, Cation distribution and magnetic properties of Zn doped NiFe2O4 nanoparticles synthesized by PEG-assisted hydrothermal route, Journal of Alloys Compound, 479 (2009) 49–55.
6. B.Lavina, Cation distribution and structure modeling of spinel solid solutions, Physical Chemistry Miner, 29 (2002) 10–18.
7. D.S.Mathew, An overview of the structure and magnetism of spinel ferrite nano particles and their synthesis in micro emulsions, Chemical Engineering. Journal, 129 (2007) 51–65.
8. S.Nazir, Structural, spectral, dielectric and photo catalytic studies of Zr-Ni doped MnFe2O4 co-precipitated nanoparticles, Ceramics International, 42 (2016) 13459–13463.
9. J.Y.Park, Ferrite-based integrated planar inductors and transformers fabricated at low temperature, IEEE Transactions on Magnetics, 33 (1997) 3322–3324.
10. N.N.Sarkar, A review of nano-ferrite synthesis and application in hyperthermia, International Journal of science and technical Research, 5 (2015) 7-12.

11. N.N.Sarkar, Cation distribution of Zn0.5Me0.5Fe2O4 (Me = Co, Ni and Cu) on the basis of rietveld refinement and magnetization measurement, Material Science Research. India, 14 (2017) 169–175.
12. N.N.Sarkar, Effect of zr^{4+} doping on curie temperature, structural and magnetic properties of Mg-Cr nano-ferrite, Indian Journal of Scientific Research, 8 (2018) 109-115.
13. N.N.Sarkar, Electrical Resistivity studies of Zr-mg doped Chromium spinel ferrites, 5 (2018) 3-11.
14. N.N.Sarkar, Structural and magnetic study of Zr^{4+} substituted magnesium ferrite Nano-particles, Journal of Physical Sciences, 22 (2017) 107-113.
15. N.N.Sarkar, Soft ferrite: a brief review on structural, magnetic behavior of nanosize spinel ferrites, Material Research Foundation, 31 (2018) 237-260.
16. N.N.Sarkar, Structural, magnetic-electrical behavior of Zr substituted Ni-Zn spinel ferrite, Resarch. Journal of Science and Technology, 10 (2018) 13-19.
17. N.N.Sarkar, Structural and magnetic studies of ($Ni_{0.5}M_{0.5}Fe_2O_4$) where M = Zn, Cu, Ferroelectrics, 519 (2017) 209–212.
18. N.T.Tayade, Perspective of distortion and vulnerability in structure by using the CdS-ZnS composite, Journal of Physical Sciences, 22(2017) 137-150.
19. M.Wang, Preparation of pure iron/Ni–Zn ferrite high strength soft magnetic composite by spark plasma sintering, Journal of Magnetic Material, 361 (2014) 166–169.
20. A.Zubair, Structural, morphological and magnetic properties of Eu-doped $CoFe_2O_4$ nano-ferrites, Results Physics, 7 (2017) 3203-3208.